Unstable resonators with 90° beam rotation

Alan H. Paxton and William P. Latham, Jr.

Unstable resonators with 90° beam rotation are discussed. Geometric properties of the forward and reverse modes are derived, and diffractive-optical properties are described. An equation for the equivalent Frensel number is obtained. Plots of eigenvectors of the resonator integral equation are included, and the equivalence of these resonators to a type of strip resonator is established.

I. Introduction

Conventional unstable resonators are not well suited for use with lasers that have low round-trip gain, because the outcoupled beam would have a thin annular cross-sectional shape which would propagate with a large angular divergence and would only focus to a far less intense spot than would be obtained from a filled-in beam with the same outer radius and total power.[1] The configurations that have been suggested to improve the far-field performance of moderate-gain lasers all have undesirable properties. For example, the unstable resonator with radially varying magnification requires the use of aspherical mirrors.[2,3]

Unstable resonators with beam rotation can be configured so that the output beam is unobscured.[4,5] The resonator with 90° beam rotation (UR90), which was proposed in Ref. 6, has a filled-in output beam which is rectangular. UR90 has the drawback that the geometric feedback power ratio determines the ratio of the two transverse dimensions of the laser mode, if spherical optical elements are used. Moreover, in most cases, ring–resonator configurations will be required to avoid excessive power loss on the back of the scraper mirror. Another difficulty with a standing-wave configuration is that the beams traveling in the two directions will overlap so that their combined outline is not a rectangle. Nevertheless, it is likely that UR90 will be useful in a variety of lasers. Unstable resonators with beam rotation have the added advantage that aberrations due to index-of-refraction variation in the gain medium or imperfect optical elements are mitigated.[7,8]

The bare-cavity mode equations for this resonator have an unusual property. They reduce to a 1-D eigenvalue problem with a 1-D solution specifying the mode in both transverse dimensions.[6,9]

II. Elementary Geometric Properties

It is well known that beam rotation occurs in a traveling-wave resonator in which the optical axis is not contained in a single plane[10] or in a standing-wave resonator with two end mirrors, each consisting of a roof–mirror assembly.[5] Beam rotation has been used to decrease the beam quality degradation due to optical-path-length variations of mode rays within lasers.[7,8]

Beam rotation, or image rotation, in an unstable resonator occurs as follows: A ray of the mode starts at location r,ϕ of the feedback mirror plane (a plane transverse to the optical axis near the feedback mirror), as shown in Fig. 1. After the ray has traced a round trip through the resonator, it crosses the feedback mirror plane at location Mr, $\phi + \phi_b$, where M is the resonator magnification and ϕ_b is the beam-rotation angle. Thus the rays spiral out from the optical axis as they complete a number of round-trip passes within the resonator.

An unstable ring resonator is illustrated in Fig. 2. The beam is rotated 90° and magnified by magnification M during one round trip. The output beam is outcoupled by an effectively semi-infinite scraper mirror. An end view of the beam at the scraper plane is illustrated in Fig. 3. Beam *abde* arrives at the scraper mirror plane. The dashed line is the outline of the scraper mirror. Beam *cdef* strikes the scraper mirror and is outcoupled. Beam *abcf* is fed back into the resonator. During a round trip through the resonator, beam *abcf* is rotated clockwise 90° about the optical axis, point *o*, and is magnified by M. The bottom edge of the feedback mirror is distance a from the optical axis. After the beam is rotated, this edge becomes the left side, and after magnification it is distance Ma from

Alan H. Paxton is with Mission Research Corporation, 1720 Randolph Road, S.E., Albuquerque, New Mexico 87106; and William Latham is with U.S. Air Force Weapons Laboratory, Kirtland Air Force Base, New Mexico 87117.

Recevied 27 January 1986.

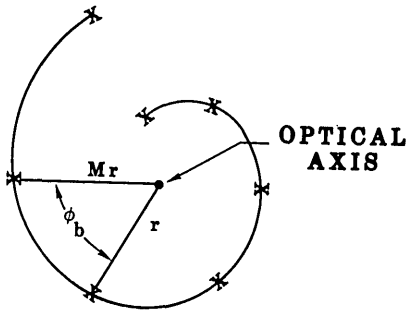

Fig. 1. Locations X that a ray of the mode of an unstable resonator with beam rotation pierces a transverse plane during a number of passes. (The beam rotation angle is ϕ_b, and the resonator magnification is M).

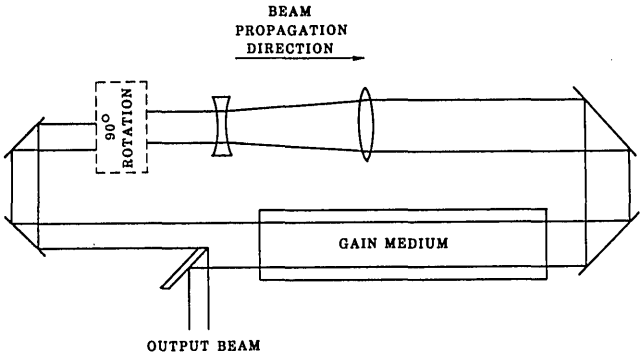

Fig. 2. Ring resonator with 90° beam rotation. A rectangular output beam is scraped off one side of the resonator beam.

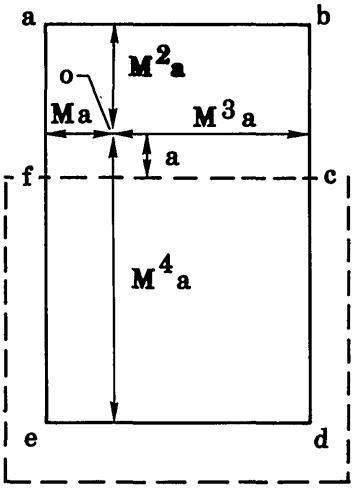

Fig. 3. Cross section of the beam at the scraper plane.

the optical axis. After magnification and rotation, the width-to-height ratio is $1/M$. Immediately after the beam is fed back, this ratio is M. Therefore, the cavity feedback-power ratio, which depends mainly on M, determines the beam shape.

An extra degree of freedom to vary the resonator feedback-power ratio independently of the width-to-height ratio of the beam traveling through the gain medium may be obtained through use of unequal magnification in the two transverse directions. An end view of the beam is illustrated in Fig. 4. The beam passes the scraper edge, and beam $abcf$ is fed back. The beam is then rotated 90° in the clockwise direction and then magnified by M_x in the horizontal direction and M_y in the vertical direction before returning to the scraper plane. The effective magnification of the resonator is $\sqrt{M_xM_y}$, and the width-to-height ratio is $1/M_y$ immediately before the beam reaches the scraper and is M_x immediately after the beam is fed back. The unequal magnification in the two directions may be obtained by using a telescope that includes spherical and cylindrical mirrors, or astigmatism may be deliberately introduced using tilted spherical mirrors.[11,12]

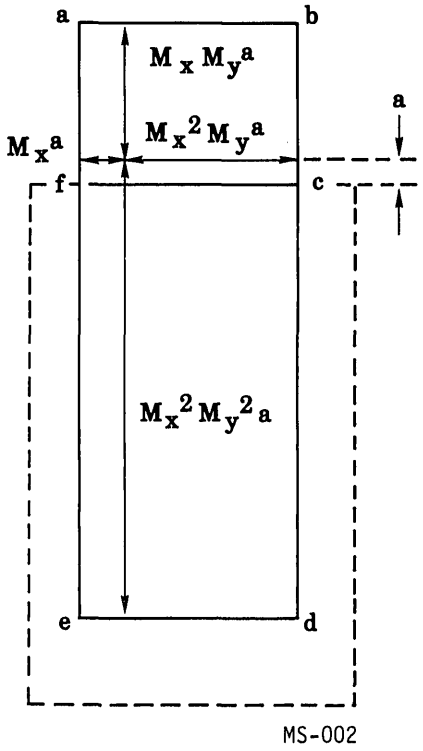

Fig. 4. Cross section of the beam of a resonator with different magnification in the two transverse directions.

The resonator mode is topologically similar to a loop with a square cross section that has a 90° twist before it closes on itself (Fig. 5). The scraped edge of the beam becomes each other edge on subsequent passes until it returns to the scraper again. In this sense, the beam has one straight geometric boundary, which arrives at the scraper every fourth pass.

An important property of unstable resonators with beam rotation is the possibility of a diffraction-limited output beam, even for a resonator with $M_y > 1, M_x = 1$. In sharp contrast to a similar resonator without beam rotation, the geometric sensitivity to tilt of the mirrors in either direction is finite; an optical axis still exists. The transverse mode discrimination does not necessarily deteriorate if $M_x = 1$, because the mode eigenvalues do not depend on M_x and M_y individually (except as they affect the equivalent collimated propagation distance for the mode) but on the product M_xM_y.

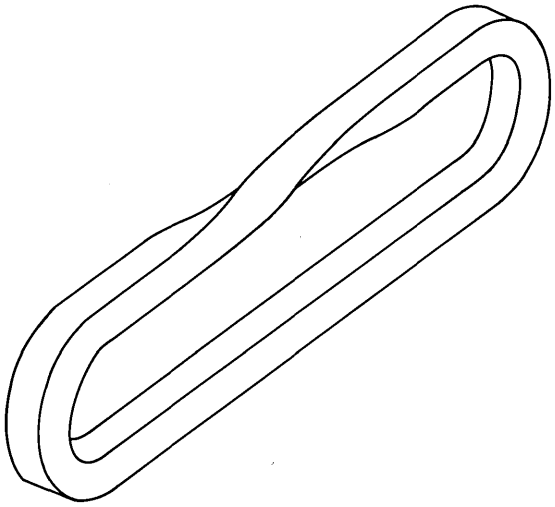

Fig. 5. Twisted loop with a square cross section has a topology similar to the ring resonator with 90° beam rotation.

III. Extended Matrix Formulation for Analyzing Nonorthogonal Unstable Resonators

The canonical formulation for unstable resonators was presented by Siegman.[13] It consists of a 2 × 2 matrix formulation of paraxial ray optics. The results of a 2 × 2 matrix analysis for unstable resonators are the geometric beam sizes, the geometric eigenvalues which are related to the resonator magnification, the geometric curvature for the eigenstates, and the collimated and equivalent Fresnel numbers for the resonator which are related to the effects of diffraction in the resonator. Gerrard and Burch[14] showed how the 2 × 2 matrix formulation could be extended to a 3 × 3 matrix formulation to include decentration and tilt in a single meridional plane in the resonator. For the resonators considered in this paper, it is necessary to include the capability to treat tilt and decentration in two orthogonal planes as well as the capability to rotate the rays in a transverse plane of the resonator. We, therefore, apply the extended 5 × 5 ray matrices defined in Ref. 9. The ray matrix for a round-trip propagation in a resonator has the form

$$R \equiv \begin{pmatrix} A_x & B_x & P & Q & d_x \\ C_x & D_x & R & S & \theta_x \\ T & U & A_y & B_y & d_y \\ V & W & C_y & D_y & \theta_y \\ 0 & 0 & 0 & 0 & 1 \end{pmatrix} = \left(\begin{array}{cc|c|c} \Theta_x & & p & d_x \\ & & & \theta_x \\ \hline q & & \Theta_y & d_y \\ & & & \theta_y \\ \hline 0\ 0 & & 0\ 0 & 1 \end{array}\right), \tag{1}$$

where we have identified four 2 × 2 blocks in the 5 × 5 operator. We assume that the symmetry axes of any astigmatic optical elements are aligned with the x and y axes.

If the resonator is orthogonal, by definition all elements of p and q are zero, and the 2 × 2 operators, Θ_x and Θ_y, are the usual ABCD matrices in the 2 × 2 formulation of the unstable resonator.[15] The x and y elements are not necessarily equal so that toroidal or cylindrical mirrors may be treated. The two off-diagonal blocks p and q are terms which mix the elements of the ray vector corresponding to the x and y coordinates. p and q contain elements only if beam rotation is included because of the assumption that the axes of symmetry of any astigmatic elements are aligned with x and y axes.[15] The fifth column in the matrix includes the x and y decentration terms, d_x and d_y, which act to displace a ray along x and y and tilt terms, θ_x and θ_y, which tilt the ray with respect to the reference axis.

A coordinate system may be defined so that beam rotation is considered to take place at a single plane within the resonator. The beam rotation matrix is[9]

$$\begin{pmatrix} \cos\phi & 0 & -\sin\phi & 0 & 0 \\ 0 & \cos\phi & 0 & -\sin\phi & 0 \\ \sin\phi & 0 & \cos\phi & 0 & 0 \\ 0 & \sin\phi & 0 & \cos\phi & 0 \\ 0 & 0 & 0 & 0 & 1 \end{pmatrix}. \tag{2}$$

The 5 × 5 matrix R operates on a five-component ray vector V given by

$$\mathbf{V} = \begin{pmatrix} r_x \\ r_x' \\ r_y \\ r_y' \\ 1 \end{pmatrix}, \tag{3}$$

where r_x and r_y are the ray heights from the reference axis along the x and y axes, respectively, and r_x' and r_y' are the angles that the ray makes with the reference axis in the x and y plane.

The eigenvalues and eigenvectors for the matrix R are given by

$$\mathrm{R}\mathbf{V}_\lambda = \lambda \mathbf{V}_\lambda, \tag{4}$$

where $\mathbf{V}_\lambda$ is the ray eigenvector for the eigenvalue λ. For a perfectly aligned resonator without beam rotation, the usual eigenvalues for the two transverse directions are obtained:

$$\lambda = M_x,\ \frac{1}{M_x},\ M_y,\ \frac{1}{M_y},\ 1.$$

These are the eigenvalues for Θ_x and Θ_y plus the solution $\lambda = 1$, which occurs because of the lower right-hand element of R. The eigenvalues corresponding to the rays of the resonator mode are M_x and M_y, while the eigenvalues $1/M_x$ and $1/M_y$ correspond to the resonator converging wave, and $\lambda = 1$ corresponds to the optical axis. Beam rotation of 90° is the case of particular interest here. The eigenvalues are

$$\lambda = \pm i\sqrt{M_x M_y},\ \pm i/\sqrt{M_x M_y},\ 1.$$

The first two eigenvalues correspond to the resonator mode, while the second and third go with the converging wave. When there are tilts and decentrations in the resonator, the location of the optical axis is given by the eigenvector corresponding to $\lambda = 1$:

$$\mathrm{R}\mathbf{V}_A = \mathbf{V}_A. \tag{5}$$

The optical axis ray $\mathbf{V}_A$ is defined as the ray that replicates itself after a round trip through the resonator.

The ray matrix equation for a perfectly aligned resonator with 90° beam rotation can be reduced to a 2 × 2 matrix equation, and an equivalent strip resonator may be identified. The eigenvalue equation is

$$\begin{pmatrix}\Theta_x & 0\\ 0 & \Theta_y\end{pmatrix}\begin{pmatrix}0 & -1\\ 1 & 0\end{pmatrix}\begin{pmatrix}\mathbf{V}_x\\ \mathbf{V}_y\end{pmatrix}=\lambda\begin{pmatrix}\mathbf{V}_x\\ \mathbf{V}_y\end{pmatrix}, \tag{6}$$

where

$$\mathbf{V}_x=\begin{pmatrix}r_x\\ r_x'\end{pmatrix},$$

$$\mathbf{V}_y=\begin{pmatrix}r_y\\ r_y'\end{pmatrix}.$$

Equation six separates into two coupled equations:

$$-\Theta_x\mathbf{V}_y=\lambda\mathbf{V}_x; \tag{7}$$

$$\Theta_y\mathbf{V}_x=\lambda\mathbf{V}_y. \tag{8}$$

An equation for $\mathbf{V}_x$ may be obtained from Eqs. (7) and (8),

$$-\Theta_y\Theta_x\mathbf{V}_y=\lambda^2\mathbf{V}_y. \tag{9}$$

Having solved Eq. (9) for $\mathbf{V}_y$ and λ, Eq. (7) may be solved for $\mathbf{V}_x$. Thus a resonator with 90° beam rotation is equivalent to a strip resonator with round-trip ABCD matrix $-\Theta_y\Theta_x$. The equivalent strip resonator is a negative-branch resonator with the outcoupled beam scraped from one side only.

IV. Sensitivity to Mirror Tilt

In an unstable resonator mode, the optical axis is the only ray that replicates itself after a round trip. When a resonator mirror is tilted, the optical axis is tilted or displaced (or both) at all planes within the resonator. If its displacement at the scraper plane is a sufficiently small fraction of the beam diameter, the tilt is tolerable. "A sufficiently small fraction of the beam diameter" is defined in a different way for this resonator than for a conventional resonator, because the geometric beam size of the former is determined by the separation between the scraper mirror edge and optical axis.

A drawing of the unfolded resonator is shown in Fig. 6. The round-trip 5 × 5 matrix corresponding to Fig. 6 is

$$R=\begin{pmatrix}CM_x & CL_x & -SM_x & -SL_x & \alpha_xD_x\\ 0 & C/M_x & 0 & -S/M_x & \alpha_x/M_x\\ SM_y & SL_y & CM_y & CL_y & \alpha_yD_y\\ 0 & S/M_y & 0 & C/M_y & \alpha_y/M_y\\ 0 & 0 & 0 & 0 & 1\end{pmatrix}, \tag{10}$$

where ϕ_r is the beam rotation angle,

M_x,M_y are magnification values in the two transverse dimensions,

α_x,α_y are beam tilt angles in two transverse directions introduced at distance L_1 past the plane of the scraper mirror, and

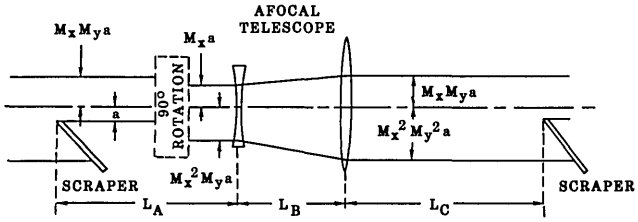

Fig. 6. Unfolded resonator.

$$L_1+L_2=L_A$$

$$S=\sin\phi_r,\ C=\cos\phi_r,$$

$$L_x=M_x(L_1+L_2)+L_B+L_C/M_x,$$

$$L_y=M_y(L_1+L_2)+L_B+L_C/M_y,$$

$$D_x=M_xL_2+L_B+L_C/M_x,$$

$$D_y=M_yL_2+L_B+L_C/M_y.$$

The optical axis location and tilt are given by the eigenvector of R with eigenvalue 1. Our main interest is in the case with $\phi_r=90°$, for which the eigenvector elements are as follows:

optical axis displacements at scraper,

$$V_1=r_x=\{\alpha_x[D_x(1+M_xM_y)-L_x-L_yM_xM_y]+\alpha_yM_x[L_y-L_x-D_y(1+M_xM_y)]\}/(1+M_xM_y)^2, \tag{11}$$

$$V_3=r_y=\{\alpha_xM_y[L_y-L_x+D_x(1+M_xM_y)]+\alpha_y[D_y(1+M_xM_y)-L_y-L_xM_xM_y)]\}/(1+M_xM_y)^2; \tag{12}$$

optical axis tilts at scraper,

$$V_2=r_x'=(\alpha_xM_y-\alpha_y)/(1+M_xM_y), \tag{13}$$

$$V_4=r_y'=(\alpha_x-\alpha_yM_x)/(1+M_xM_y). \tag{14}$$

The distance from the optical axis to the scraper mirror determines the geometric beam size; so, to maintain the correct beam size, r_y should be a small fraction of the desired value for this distance. Similarly, r_x must be a small fraction of the beamwidth to avoid losing part of the beam on apertures around the gain medium.

V. Integral Equation for Bare-Cavity Modes

A resonator with 90° beam rotation has the property that the bare-cavity mode in both transverse dimensions corresponds to a single eigenvalue.[6,9] This differs fundamentally from the bare-cavity mode of a resonator without beam rotation, which is determined by two independent eigenvalues corresponding to the two transverse dimensions.

The integral for propagation from the plane of the scraper mirror back to the plane of the scraper mirror for a resonator like the one illustrated in Fig. 6, but without beam rotation is

$$w(x,y)=\int K(x,y,x',y')w'(x',y')dx'dy', \tag{15}$$

where $w'(x',y')$ is the scalar field amplitude before

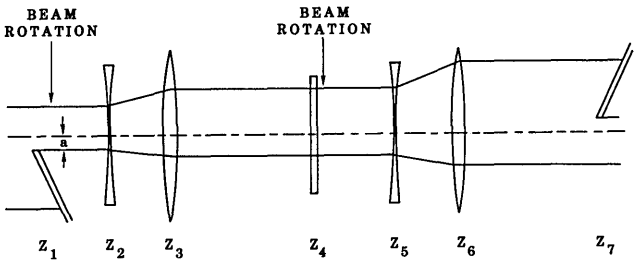

Fig. 7. Unfolded and untwisted resonator—two passes.

propagation, and $w(x,y)$ is the field after propagation. The kernel is separable into the product

$$K(x,y,x',y') = K_1(x,x')K_2(y,y'). \tag{16}$$

We assume that the fields are separable for a resonator with 90° beam rotation.

$$w(x,y) = u(x)v(y). \tag{17}$$

Incorporating 90° beam rotation, Eq. (15) becomes

$$v(y) = \int_{-a}^{\infty} K_1(y,x')u'(x')dx', \tag{18}$$

$$u(x) = \int_{-\infty}^{\infty} K_2(-x,y')v'(y')dy'. \tag{19}$$

Equations (18) and (19) may be combined to give

$$u(x) = \int_{-a}^{\infty} C(x,x')u''(x')dx', \tag{20}$$

where

$$C(x,x') = \int_{-\infty}^{\infty} K_2(-x,y)K_1(y,x')dy,$$

which is the equation for the propagation of $u''(x')$ two passes through the resonator. The equation for the resonator modes is

$$\lambda_i u_i(x) = \int_{-a}^{\infty} C(x,x')u_i(x')dx', \tag{21}$$

and the y dependence is obtained using Eq. (18),

$$v_i(y) = \int_{-a}^{\infty} K_1(y,x)u_i(x)dx. \tag{22}$$

The kernel for the resonator equation is the propagation kernel for a two-pass transit of the unfolded and untwisted resonator shown in Fig. 7. Examination of the eigenvalue equation, Eq. (21), indicates that the rectangular-beam resonator with 90° beam rotation is equivalent to a negative-branch strip resonator with an outcoupling scraper mirror on only one side of the beam rather than on both.

VI. Numerical Calculation of Bare-Cavity Modes

The kernel of the integral of Eq. (21) involves an equivalent collimated Fresnel number[16] that may be obtained from Fig. 7. Propagation distances with constant centers of curvature are $L_1 = Z_2 - Z_1$, $L_2 = Z_3 - Z_2$, $L_3 = Z_5 - Z_3$, $Z_6 - Z_5 = L_2$, and $L_4 = Z_7 - Z_6 = Z_4 - Z_3$. The equivalent collimated propagation distance for the untwisted double-pass transit shown in Fig. 7 is

$$L_{eq} = L_1 + L_2(1/M_x + 1/M_x^2M_y) + L_3/M_x^2 + L_4/M_x^2M_y^2. \tag{23}$$

The equivalent collimated propagation distance corresponding to the kernel $K_1(y,x')$ is

$$L'_{eq} = L_1 + L_2/M_x + L_4/M_x^2. \tag{24}$$

In terms of Fig. 6, these equations are

$$L_{eq} = L_A(1 + 1/M_x^2) + L_B(1/M_x + 1/M_x^2M_y) \tag{25}$$

$$+ L_c(1/M_x^2 + 1/M_x^2M_y^2), \tag{25}$$

$$L'_{eq} = L_A + L_B/M_x + L_c/M_x^2. \tag{26}$$

The kernel of Eq. (21) is

$$C(x,x') = \left(1/\sqrt{iM\lambda L_{eq}}\right) \exp\left[\frac{i\pi}{\lambda L_{eq}}(x' + x/M)^2\right], \tag{27}$$

where $M = M_xM_y$, and

$$K_1(y,x') = \left(1/\sqrt{iM_x\lambda L'_{eq}}\right) \exp\left[\frac{i\pi}{\lambda L'_{eq}}(x' + y/M_x)^2\right]. \tag{28}$$

The coordinates of the optical axis have values $x_0 = 0$, $y_0 = 0$. We define the collimated Fresnel number

$$N = a^2/\lambda L_{eq}. \tag{29}$$

The matrix equation obtained by substituting the Fresnel-Kirchhoff kernels in Eq. (21) and discretizing the result is

$$\lambda_i \mathbf{v}_i = P\mathbf{v}_i, \tag{30}$$

where

$$P_{jk} = (f/iM)^{1/2} \exp[i\pi f[(j - n)/M + k - n]^2], \tag{31}$$

$$f = N/n^2.$$

The index of the optical axis is n. The matrix had a large enough dimension so that during the calculations the beam was not clipped significantly on the side opposite the scraper mirror. The eigenvalues and eigenvectors of the matrix [Eq. (31)] were calculated using a standard numerical procedure.

We calculated the modes for $N = 3.78$ and $M = 1.86$. The intensity and phase of the lowest-loss mode are shown in Figs. 8 and 9. The x-coordinate and y-coordinate values are normalized so that the distance from the scraper mirror edge to the optical axis is equal to 1. The phase variation is insignificant across the geometric beam, and the intensity has three main peaks. The field distribution in the other transverse direction was calculated using a discretized version of Eq. (18). The Fresnel number

$$N' = a^2/\lambda L'_{eq} \tag{32}$$

was given the value $N' = 5.39$. The field distribution in the other transverse dimension is shown in Figs. 10 and 11. The phase is also adequately flat in this dimension to allow nearly diffraction-limited beam quality.

The magnitude of the eigenvalue of the lowest loss mode was found to be $|\lambda_1| = 0.792$, and the next largest eigenvalue had magnitude $|\lambda_2| = 0.540$. This separa-

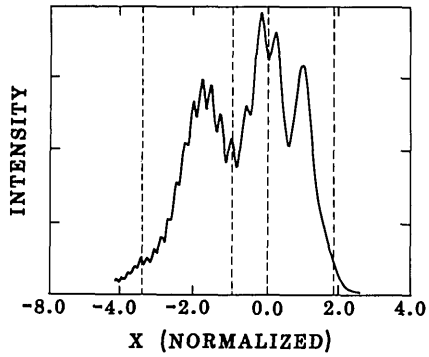

Fig. 8. Intensity of bare-cavity lowest loss mode at the scraper–mirror plane. (The optical axis is at $X = 0.0$. The dashed line just to the left of the optical axis is the scraper edge location. The other two dashed lines are at the geometric edges of the beam.)

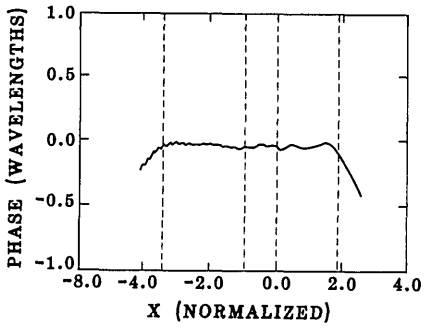

Fig. 9. Phase of lowest loss bare-cavity mode.

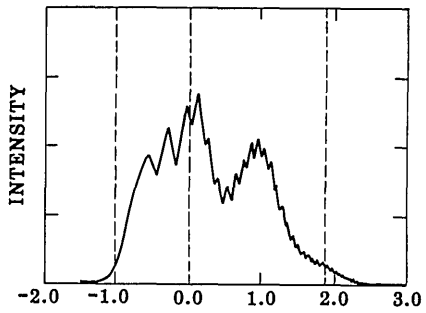

Fig. 10. Mode intensity at output plane, bare cavity.

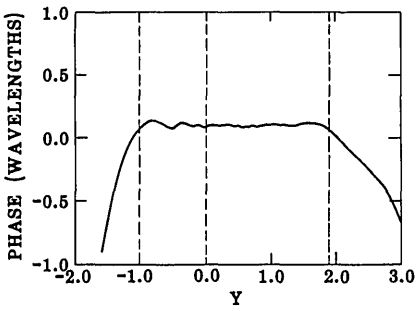

Fig. 11. Mode phase at output plane, bare cavity.

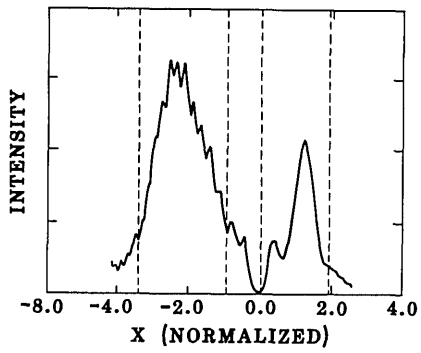

Fig. 12. Intensity of second lowest loss mode.

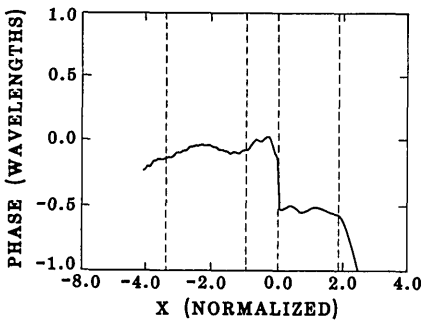

Fig. 13. Phase of second lowest loss mode.

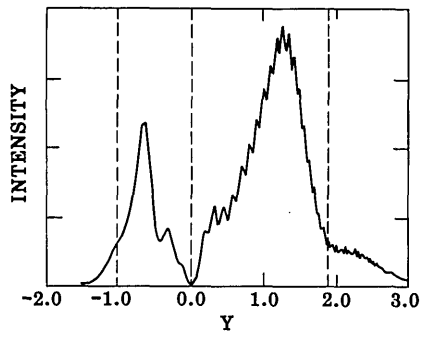

Fig. 14. Intensity of second lowest loss mode.

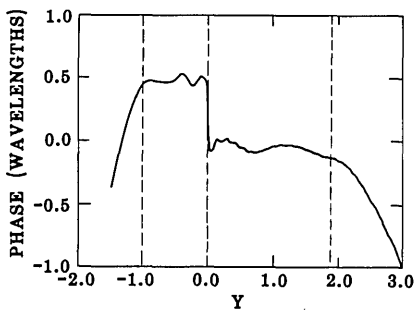

Fig. 15. Phase of second lowest loss mode.

tion should ensure laser operation in a single transverse mode.

The second-lowest-loss mode is shown in Figs. 12–15. There is a π phase jump at the optical axis in each transverse dimension. A mode with essentially uniform phase in one transverse coordinate and with large phase variation in the other is not possible in a resonator with 90° beam rotation, although it is possible in a conventional unstable resonator. The resonator se-

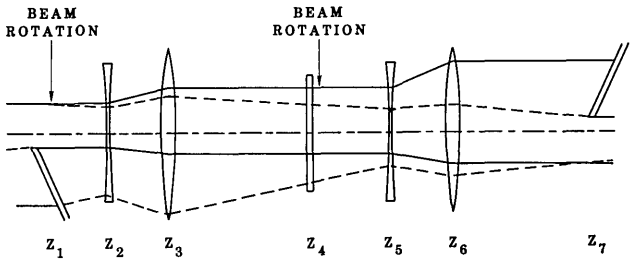

Fig. 16. Untwisted and unfolded resonator. (Dashed line is geometric edge of reverse mode.)

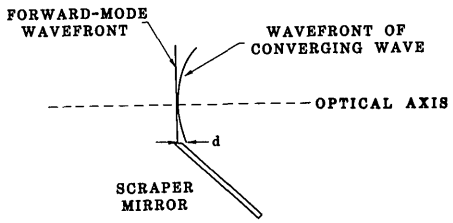

Fig. 17. Equivalent Fresnel number is determined from the distance between the edge of the scraped forward wave front and the wave front of the resonator converging wave.

lected for a sample case is very likely to operate with nearly diffraction-limited beam quality.

VII. Reverse Mode

A sketch of the unfolded and untwisted resonator is shown in Fig. 16. The geometric edge of the reverse mode is drawn with dashed lines. A reverse-mode suppressor mirror may be placed at some convenient location to suppress the reverse mode by retroreflecting some of its light into the forward direction.[17] It may be desirable to use a roof mirror in combination with a curved mirror or a lens to allow an even number of reflections before the output of the reverse beam is injected in the forward direction.[18] Although Fig. 16 would seem to indicate that the best location for the retro mirror is the back of the scraper mirror, in practice, apertures within the resonator will probably alter this situation. In a plane orthogonal to the scraper mirror edge, the radius of curvature of the reverse mode at the scraper mirror is

$$R_r = M_x^2 M_y^2 L_{eq}/(M_x^2 M_y^2 - 1). \tag{33}$$

VIII. Equivalent Fresnel Number

The equivalent Fresnel number[19,20] is obtained using the prescription of Ref. 21. A plane wave front of the forward mode and a wave front of the converging wave are illustrated in Fig. 17. The distance d from the converging wave to the edge of the scraped forward-mode wave front, if they just touch at the optical axis, is used to determine the equivalent Fresnel number,

$$N_{eq} = d/\lambda. \tag{34}$$

The converging wave is simply the time-reversed reverse wave, so Eq. (33) may be used to obtain

$$N_{eq} = \frac{a^2(M_x^2 M_y^2 - 1)}{2\lambda M_x^2 M_y^2 L_{eq}}. \tag{35}$$

The same equation was derived using paraxial ray matrices in Ref. 9. The value corresponding to our calculated example is $N_{eq} = 1.35$. A value close to 1.5 is suggested by the three peaks in the intensity distribution of the lowest loss mode.

IX. Concluding Remarks

Because the apertured edge of the feedback beam must make four passes through the resonator before it is clipped again, diffractive spreading may become a problem for UR90. The equivalent Fresnel number may be increased by replacing the positive-branch afocal telescopes shown in the illustrations with negative-branch telescopes, which have internal foci. It may be desirable to configure some resonators to have infinite equivalent Fresnel numbers.[22]

We are indebted to A. Gavrielides of the Air Force Weapons Laboratory for suggesting that a rectangular resonator geometry analogous to Ananev's spiral would be interesting to consider. This work benefited from several discussions with M. E. Rogers of the Air Force Weapons Laboratory. We are grateful to A. E. Siegman for sending us a section of his book *Lasers*[15] prior to publication. The part of this work that was done at Mission Research Corp. was funded by the U.S. Air Force, Air Force Systems Command, Air Force Weapons Laboratory at Kirtland AFB, NM.

References

1. D. A. Holmes, J. E. Korka, and P. V. Avizonis, "Parametric Study of Apertured Focused Gaussian Beams," Appl. Opt. **11**, 565 (1972).
2. T. R. Ferguson and M. E. Smithers, "Optical Resonators with Nonuniform Magnification," J. Opt. Soc. Am. **A 1**, 653 (1984).
3. M. E. Smithers and T. R. Ferguson, "Unstable Optical Resonators with Linear Magnification," Appl. Opt. **23**, 3718 (1984).
4. Yu. A. Ananev, *Optical Resonators and the Problem of Divergence of Laser Emissions* (Izdatelstvo, Moscow, 1979).
5. Yu. A. Ananev, "Unstable Laser Resonator for Low-Gain Media," Sov. Tech. Phys. Lett. **4**, 150 (1978).
6. V. N. Kuprenyuk, V. E. Semenov, L. D. Smirnova, and V. E. Sherstobitov, "Wave-Approximation Calculation of an Unstable Resonator with Field Rotation," Sov. J. Quantum Electron. **13**, 1613 (1983).
7. Yu. K. Danileiko and V. A. Lobachev, "New Rotating-Field Resonator for Lasers," Sov. J. Quantum Electron. **4**, 389 (1974).
8. D. L. Bullock, D. N., Mansell, and S. G. Forbes, "Azimuthal Mode Control for Lasers," U.S. Patent 4,011,523 (8, Mar. 1977).
9. A. H. Paxton and W. P. Latham, Jr., "Ray Matrix Method for the Analysis of Optical Resonators with Image Rotation," Proc. Soc. Photo-Opt. Instrum. Eng. **554**, 159 (1985).
10. J. A. Arnaud, "Degenerate Optical Cavities," Appl. Opt. **8**, 189 (1969).
11. P. Hoffmann, "Confocal Unstable Optical Resonator with Asymmetrical Magnification," Opt. Lett. **6**, 598 (1981).
12. C. Cason, R. W. Jones, and J. F. Perkins, "Unstable Optical Resonators with Tilted Spherical Mirrors," Opt. Lett. **2**, 145 (1978).
13. A. E. Siegman, "A Canonical Formulation for Analyzing Multielement Unstable Resonators," IEEE J. Quantum Electron. **QE-12**, 35 (1976).

14. A. Gerrard and J. M. Burch, *Introduction of Matrix Methods in Optics* (Gersham Press, Old Woking, Surrey, England, 1975).
15. A. E. Siegman, *Lasers* (University Science Books, Mill Valley, California, 1986).
16. E. A. Sziklas and A. E. Siegman, "Mode Calculation in Unstable Resonators with Flowing Saturable Gain. 2: Fast Fourier Transform Method," Appl. Opt. **14**, 1874 (1975).
17. R. J. Freiberg, P. P. Chenausky, and C. J. Buczek, "Asymmetric Unstable Traveling-Wave Resonators," IEEE J. Quantum Electron. **QE-10**, 279 (1974).
18. G. C. Dente and C. L. Clayton [U.S. Air Force Weapons Laboratory; private communications] regarding the injection of a nonresonant beam in the forward direction if the usual combination of scraper and suppressor mirrors is used.
19. A. E. Siegman and R. Arrathoon, "Modes in Unstable Optical Resonators and Lens Waveguides," IEEE J. Quantum Electron. **QE-3**, 156 (1967).
20. A. E. Siegman and H. Y. Miller, "Unstable Optical Resonator Loss Calculations using the Prony Method," Appl. Opt. **9**, 2729 (1970).
21. Yu. A. Ananev, "Unstable Resonators and Their Applications," Sov. J. Quantum Electron. **1**, 565 (1972).
22. A. H. Paxton and T. C. Salvi, "Unstable Optical Resonator with Self Imaging Aperture," Opt. Commun. **26**, 305 (1978).

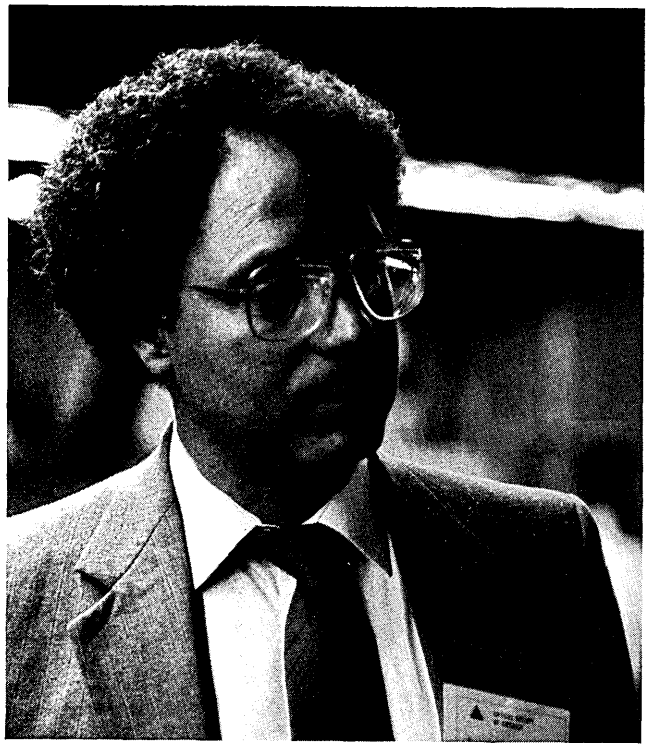

B. Feldman of the Naval Research Laboratory, Washington, DC, photographed by W. J. Tomlinson of Bell Communications Research—Red Bank, at the 1985 OSA Annual Meeting in Washington, DC.

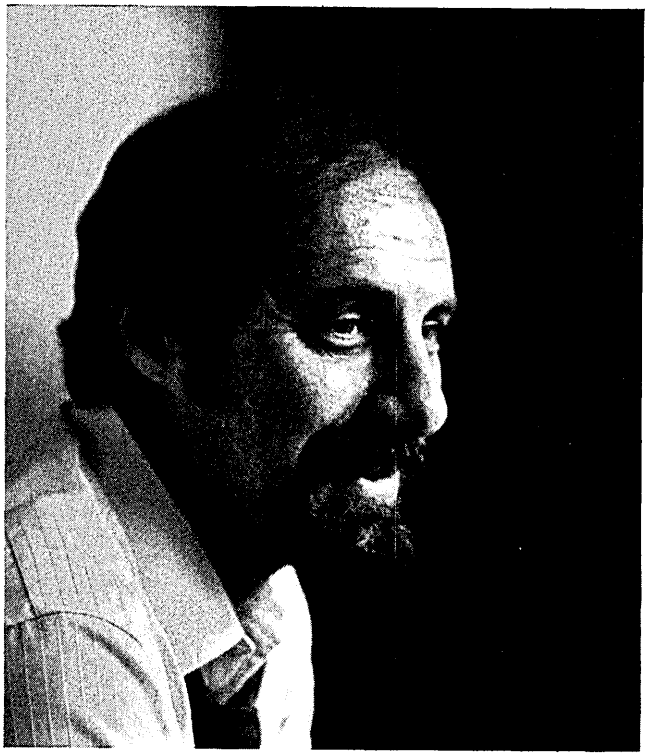

John G. Kepros of the *Applied Optics* Patents Panel photographed by W. J. Tomlinson of Bell Communications Research—Red Bank, at the 1985 OSA Annual Meeting in Washington, DC.